Modification of electronic states of solvent sensitive probes by vibrational strong coupling

Yogendra Sharma

A dissertation submitted for the partial fulfilment of
BS-MS dual degree in Science

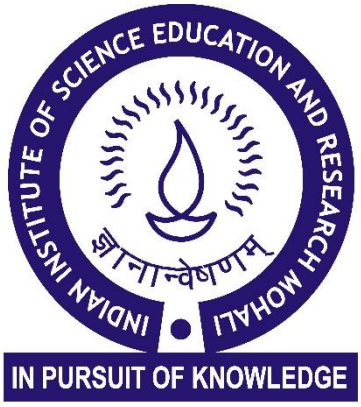

Indian Institute of Science Education and Research Mohali

April 2019

Certificate of Examination

This to certify that the dissertation titled **"Modification of electronic states of solvent sensitive probes by vibrational strong coupling"** submitted by **Mr. Yogendra Sharma** (Reg. No. MS14147) for the partial fulfilment of BS-MS dual degree programme of the Institute, has been examined by the thesis committee duly appointed by the Institute. The committee finds the work done by the candidate satisfactory and recommends that the report be accepted.

Dr. Arijit K. De Dr. P. Balanarayan Dr. Jino George

(Supervisor)

Dated:

Declaration

The work presented in the dissertation has been carried by me under the guidance of Dr. Jino George at the Indian Institute of Science Education and Research Mohali.

This work has not been submitted in part or in full for a degree, or diploma, or a fellowship to any other University or Institute. Whenever contribution of others are involved, every effort is made to indicate this clearly, with due acknowledgement of collaborative research and discussions. This thesis is a bonafide record of original work done by me and all sources listed within have been detailed in bibliography.

Yogendra Sharma

(Candidate)

Dated:

In my capacity as the supervisor of the candidate's project work, I certify that the above statements by the candidate are true to the best of my knowledge

Dr. Jino George

(Supervisor)

Acknowledgement

Without acquiring any help from others, nobody succeeds in any field. I would like to acknowledge all people, who directly or indirectly contributed to my MS thesis. I am very lucky to have **Dr. Jino George** as my MS thesis supervisor. In many occasions, he has given valuable suggestions that directed me towards right path and motivated me for learning new concepts. His understating and positive approach towards problems, his enormous conviction and intellectual ideas make him best supervisor. I am feeling blessed for submitting my thesis under his supervision.

I would like to thank my thesis committee members Dr. Arijit K. De and Dr. P. Balanarayan for their valuable inputs and support.

My sincere thanks to Ms. Jyoti Lather and Ms. Pooja Bhatt for helping me during the project work and for their fruitful suggestions during thesis writing. I cannot avoid my other lab members Ms. Kripa M. Joseph, Ms. Akhila Kadyan and Mr. Jaibir who helped in some or other way throughout my project work. They made my life pleasant with lively and consenting environment.

I am thankful to IISER Mohali for providing me the instrumental and other infrastructural facilities during the course of my project.

At last, I would like to my parents, my brothers and my friends Mr. Suresh Kumar, Mr. Tinku Ram Meena, Mr. Apoorv Alawada, Mr. Shubham Bhojane and Mr. Ravi Kumar for thesis motivation to accomplish my work.

List of figures

List of Tables

Notations

$\hbar\Omega_R$ = Rabi splitting

λ = Wavelength of light

ANS = Anilinonapthalenesulphonates

$\sqrt{C}$ = Square root of concentration

E_F = Fluorescence energy

E_T30 = Solvent polarity energy

F–P cavity = Fabry-Perot cavity

FSR = Free spectral range

IR = Infrared

P+ and P- = Polaritonic states

V_n = Vibrational level

VSC = Vibrational Strong Coupling

Abstract

In the recent years both experimental and theoretical studies observed that chemical reaction landscape can be sculpted preciously by selective vibrational strong coupling (VSC) of reactant molecules. In VSC, excited vibrational state undergoes strong coupling with IR photons (cavity modes) which leads to the formation of hybrid light-matter states known as vibro-polaritonic state (P+ and P-). In the current project, we have studied the modification of energy levels of a solvent sensitive probe, 8-Anilinonaphthalene-1-sulfonic acid (1,8-ANS) under VSC of the solvent system. It has been observed that 1,8-ANS is very sensitive to solvent environment, specifically presence of water can modify both the radiative and non-radiative decay rates of the molecules. By changing the water composition, the electronic transition energy (solvatochromism) of 1,8-ANS also getting modified. Here, we observed the fluorescence behaviour of 1,8-ANS molecule are affected by VSC of O-H stretching mode of water molecules. Concentration dependent studies show that the shift in the electronic transition energy is completely different from the non-cavity conditions. These observations open up new questions on the application of VSC for controlling bulk properties like solvent polarity and also on the modification of intrinsic behaviour of associated chromophoric systems.

Contents

Chapter 1: Introduction

1.1 Historical Background

It has been of great interest for the scientific community to achieve multifunctional systems by modulating the chemical and the physical properties of the molecules and materials. In chemistry, changes in the properties are mainly achieved through chemical modification. Whereas, physical forces such as dispersion force play a crucial role in controlling the state of a system. For e.g., London dispersion forces can change He-atom from gaseous to liquid state at 4 K. Hence, weak interaction lay the foundation of universe by controlling matter-matter interactions

In the same line, "Forster Resonance Energy transfer" (FRET)-weak interaction-is a classic example of a second order dipole-dipole coupling. In 1948, Forster proposed that the energy transfer can take place between the donor-acceptor conformers by the transition dipole-dipole interaction through space[1]. If the emission spectra of the donor overlaps with the absorption spectra of the acceptor (on resonance condition) and the distance between the donor-acceptor conformers is small enough, the Coulomb interaction between the transition dipole moments become significant that lead to funnelling of energy from donor to acceptor molecules. It also depends on the relative orientation and magnitude of the transition dipole moment of the conformers. On the other side, in exciton coupling, a first order dipole-dipole interaction occurs between similar or dissimilar molecules that lead to reshuffling of their energy levels. At higher concentrations, organic dye molecules can self-aggregates, which alters their molecular states with defined Eigen states which in turn leads to either the red shift (J-aggregates) or blue shift (H-aggregate) depending upon the symmetry of the dipoles.[2] (figure 1.1)

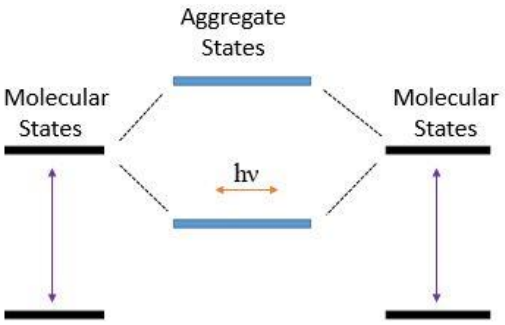

Figure 1.1: Schematic diagram of the electronic coupling between two transition dipole moments leading to the formation of the J- and H- aggregates with their new energy levels.

1.2 Light-matter strong coupling:

A) Theoretical background:

Similar to a dipole-dipole interaction a molecular transition dipole can also interact with a photonic state that leads to the formation of new energy levels in the system. This process is called as light-matter strong coupling. The strength of the light-matter interaction can be varied from weak, strong and ultra-strong depending on the coupling strength. e.g. for the weak coupling, the modification of the radiative decay rates of molecule in the vicinity of a metallic surface[3], otherwise called as Purcell effect[4]. In this sort of weak coupling only the radiative rates get affected while the system energy levels are intact. While in the strong coupling regime not only the radiative decay rates of the molecule are the one which get affected rather the entire energy levels get affected which leads to the formation of new states called polaritonic states[5]. The coupling is termed to be "strong" if the time scale of the energy transfer is faster than any other decay pathway of the molecule[6]

Classically the light-matter strong coupling problem can be looked as two different harmonic oscillators (i.e. with different masses, and different spring constant) coupled to each other with an effective spring constant. The basic approximation made to study the light-matter strong coupling is the "dipole moment approximation", which assumes that the wavelength of the light is much larger compared to the molecular length scale[7]. Another approach is to take the

quantum mechanical perspective as the strong coupling is observed in presence of vacuum field. Vacuum fluctuation or zero-point energy was first reported in the Planck's second theory of black-body radiation and Einstein's theory of molecular agitation at room temperature in 1911 and 1913 respectively[8,9]. Vacuum fluctuations are basically described as ground state energy of the quantized electromagnetic field[7]. The strength of vacuum filed (E_0) is given by:

$$E_{\circ} = \sqrt{\frac{\hbar\omega}{2\varepsilon_{\circ}\nu}} \tag{1.1}$$

where ħω is the resonant energy, $\varepsilon_{\circ}$ is the vacuum permittivity and ν is the volume of electromagnetic mode.

The quantum mechanical operator for the light-matter coupling is *V*:

$$V = -\vec{d}.\vec{E} \tag{1.2}$$

where $\vec{E}$ is electric field operator and $\vec{d}$ is the molecular dipole moment operator.

When a molecule emits light inside a cavity, the photon is reflected back and forth by the mirrors and subsequently remains inside the cavity. Therefore, the probability of reabsorption by the molecule is enhanced. If this probability is higher than the probability of photon leakage through the mirror and the non-resonant decay rate of the molecule, then the system enters strong coupling[7].

B) Quantum description of strong coupling:

Light-matter strong coupling can be explained using cavity quantum electrodynamics (cQED). This system basically explains the coupling of an electromagnetic mode to one of the molecular transition modes. Here, the system is described by Jaynes-Cummings Hamiltonian[10], which describes the system as the sum of molecule, the electric field, and the molecule-field interaction within the rotating wave approximation

$$\widehat{H}_{JC} = \widehat{H}_{mol} + \widehat{H}_{cav} + \widehat{H}_{int} \tag{1.3}$$

The molecule-field interaction $\widehat{H_{int}}$ includes $g = g_{\circ}\sqrt{N}$, where g is the collective coupling. So light-matter coupling strength varies as$\sqrt{N}$. Where *N* represents the number of oscillators in

the light-matter coupling regime, so concentration of the molecule plays an important role in enhancing the coupling strength. The Jaynes-Cummings Hamiltonian can be diagonalized by the Hopfield-Bogoliubov method yielding the two eigenstates[11]. The two eigenstate are linear combinations of light and matter states, also called polaritonic states. These are designated as |P+> (higher in energy) and |P-> (lower in energy) eigen states.

$$|P^+> = \alpha|e,0> + \beta|g,1>$$

$$|P^-> = \beta|e,0> - \alpha|g,1> \quad (1.4)$$

where |g>, |e> represents the ground and excited states of the molecule respectively, and |0>, |1> the photonic states and α, β are Hopfield coefficients. The energy difference between two polaritonic states is called as the "Rabi splitting" denoted as $\hbar\Omega_R$.

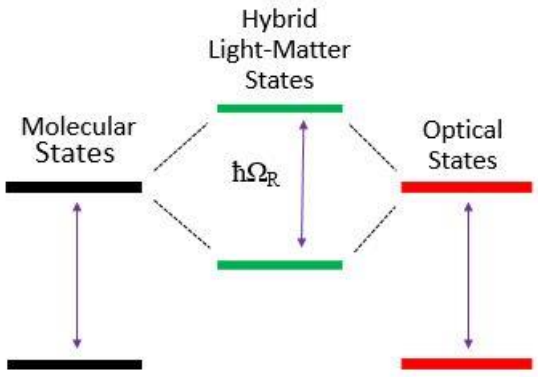

Figure 1.2: Schematic diagram of the coupling of the molecular transition dipole moment with the cavity mode (optical state), which leads to the formation of the "Hybrid Light-Matter States" also known as "polaritonic states" separated by the energy difference known as Rabi splitting ($\hbar\Omega_R$).

$$\Delta E = E_+ - E_- = \hbar\Omega_R = \sqrt{\{4V_n^2 - (\Gamma_c - \Gamma_e)^2\}} \quad (1.5)$$

where E_+ and E_- are the energies of the P+ and P- respectively, Γ_c and Γ_e are given by the decay constants ($\Gamma = \hbar/\tau$) of the photon in the cavity and the excited state respectively and V is the interaction energy of the electric component of the electromagnetic field in the cavity, $E_\circ$ and the transition dipole moment of the material, d[12] (as described in the equation (1.2)).

If all other dissipation rates are negligible than the Rabi exchange rate (from equation (1.1), (1.2) and (1.5)) then the equation can be simplified as:

$$\hbar\Omega_R = 2V_n = 2\vec{d}\cdot\overrightarrow{E_\circ} = 2d\sqrt{\frac{\hbar\omega}{2\varepsilon_\circ\nu}}\, X\,\sqrt{(n_{ph}+1)} \tag{1.6}$$

The Rabi splitting ($\hbar\Omega_R$) is directly proportional to the $\sqrt{N/\nu} = \sqrt{C}$. Form equation (1.6), it's evident that strong coupling occurs even in the dark, as $\hbar\Omega_R$ has still have a value if $n_{ph} = 0$.

The very important condition for ensuring that the system is in strong coupling is that, the splitting (Ω_R) must be larger than the full width at half maximum of the bare molecule absorption band ($\Delta\omega_x$) and the cavity mode ($\Delta\omega_c$).

$$\Omega_R > \frac{(\Delta\omega_x)+(\Delta\omega_c)}{2} \tag{1.7}$$

However the splitting alone is not the criteria for describing the system is under strong coupling, because in some instances the above (equation (1.7)) condition can be achieved in the weak coupling regime, some reasons for achieving the comparable splitting might be because of inhomogeneous broadening of the band[17] or due to the cavity induced transparency[18-20]. So in order to confirm the system is under strong coupling, the dispersive nature of polaritonic states must be confirmed (as shown in figure 4). The strength of the coupling is calculated from the ratio of the frequency (or energy) of the cavity mode to the Rabi frequency (or energy). When this ratio exceeds to 0.1 to 0.2, the system is in so called ultra-strong coupling (USC)[7]. In USC regime the energy of the coupling is significant compared to the molecular transition leading to break down of the rotating wave approximation and system need to be described within the framework of Dicke Hamiltonian[21,22]. In USC, various new process occurs, e.g. photon blockades[23,24], super radiance[25] and ground state modifications[26,27]etc.

C) Properties of polaritonic states:

(i) As already discussed, the energy difference between the polaritonic states (P+ and P-) known as Rabi splitting, is directly proportional to the square root of the number of oscillators or molecule under strong coupling. The large splitting perturbs the levels of the other molecular eigenstates that are not directly involved in in the coupling (as illustrates in figure 1.3)[12].

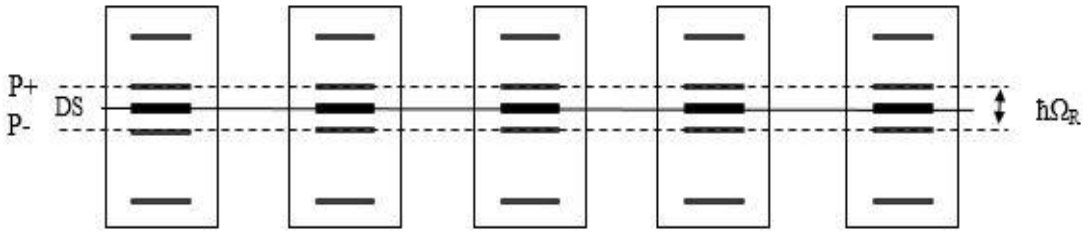

Figure 1.3: Polaritonic states, dark states (DS) delocalised over many molecules M.

The N molecules generates N+1 collective state among which two are new eigen states (P+ and P-) along with N-1 available dark state (as the transition from ground state is forbidden)[13]. Moreover, it has been shown that the emission from P- is spatially coherent over micrometre distances, resulting in interference fringes[14,15], or the molecules (which are separated by micrometre distance emit in phase[12].

(ii) As the polaritonic states are hybrid light-matter states so they have some behaviour corresponding to the light and as well as matter. So in this context, another interesting property of the polaritonic states is that they show inherent dispersive nature (momentum-energy relation) due its photonic contribution. For studying the dispersive nature, the energy of the states are plotted versus the in plane momentum ($k_{\parallel}$) (as shown in (figure 1.4), the polaritonic states formed due to the strong coupling of the O-H stretch of water). For Fabry-Perot cavity, the formula used for plotting dispersive curve:

$$|k_{\parallel}| = k_{\parallel} = \frac{2\pi}{\lambda} sin\theta \qquad (1.8)$$

where θ is the angle of incidence and λ is the peak wavelength. The Rabi splitting is defined by the minimum energy gap, where the photonic and material components are isoenergetic and contribute equally to the hybrid states. At higher $k_{\parallel}$ values, the P+ have more photonic component while P- have more material like character[12].

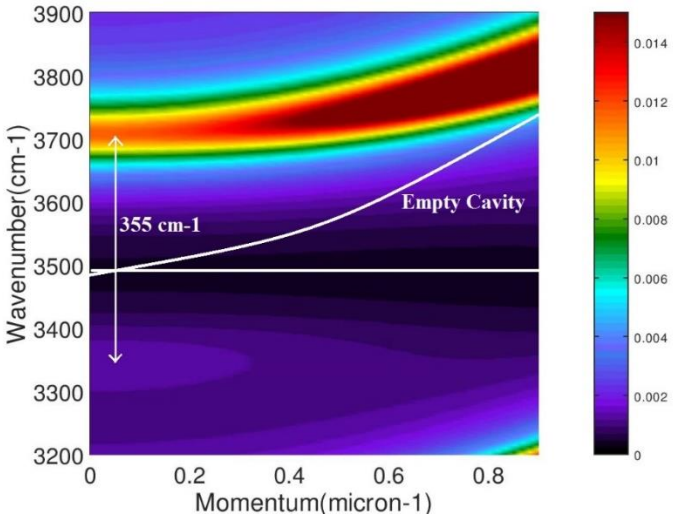

Figure 1.4: Dispersion curve of a strongly coupled Water (O-H stretch), positioned at 3500 cm^{-1}, the straight (white) line is the non-dispersive O-H absorption peak while the other white dispersive line is the empty cavity absorption peak. The Rabi splitting can be calculated from the intersection of the dispersive and non-dispersive lines.

(iii) The vacuum field is not constant in the cavity, approaching 0 at the nodes and maximum at anti-nodes. The value of Rabi splitting ($\hbar\Omega_R$) is maximized if more number of molecules are placed in the vicinity of the antinode rather than evenly spreading the molecules inside the cavity[16]. As described in equation (6), the value of ($\hbar\Omega_R$) is sensitive to the relative orientation of the $\vec{d}$ and $\overrightarrow{E_o}$, and as discussed in equation (8) the maximum interaction in case of a Fabry-Perot cavity is when molecule are aligned parallel ($k_{\parallel}$) to the electric component of the electromagnetic field, while the molecules which are aligned perpendicular ($k_{\perp}$) does not contribute to the effective coupling.

D) Vibrational strong coupling:

Light-matter strong coupling was explored very well in physics such as Bose-Einstein condensation, polariton lasing etc. Whereas, less known in terms of their effect in chemical systems. Strong coupling of molecules to the vacuum fields offers a new direction controlling molecular properties without affecting its structural behaviour. The energy landscape of a molecular system can be modified by strong coupling and it's not only affect it fundamental molecular transition but also modify the zero-point energy of the system. These modifications are reversible in nature i.e. if the molecule is moved outside of the cavity, the molecule resumes its original properties.

Light-matter strong coupling to the excited electronic states have been well explored in the last decade[28.29,69-76]. It has been proved that photochemistry and photophysics of the organic materials can be drastically changed[16] by electronic strong coupling their electronic transition[,28-30]. The kinetics of photoisomerization of spiropyran to merocyanine has been investigated in Fabry-Perot (F–P) cavity[31,32]. The photoisomerization reaction rate was observed to be decreased by 3 to 4 times. The justification for lowering reaction rate given as the energy of the P- state is lower than that of the bare molecule excited state, so now molecule has to undergo large transition energy barrier. The reason for such rate modification is due to energy level modification by strong coupling and that control the photostationary state by increasing avoided crossing in the conical intersection.

In a different attempt, Shalabney et al. showed that carbonyl vibrational band of polyvinyl acetate thin film can be effective coupled to an IR cavity photon[33]. Later, George et al. showed that vibrational strong coupling (VSC) can be achieved in molecular liquids[77]. This opened up an all set of studies to control chemical reaction by coupling to vibrational bands. The fundamental concept is the same as electronic strong coupling, here, by VSC vibro-polaritonic states are formed with a minimum vacuum splitting of $\hbar\Omega_R$ (figure 1.5). Compared to the electronic levels which are high in energy and transition involves the electrons which are delocalised over entire molecule while in the case of vibrational levels, they are low in energy and transition involves the electrons which are localised. So far vibrational strong coupling (VSC) for various molecules in both liquid and solid state have been reported, including polymers[33,34], organometallic complexes[35] and protein vibrational modes[36]. Similar to photo-

isomerization reaction control that we discussed previously, VSC can selectively control chemical reaction rate by coupling vibrational states that involved in the bond breaking/bond making process. Very recently, IISER Mohali group also observed catalysis effect by coupling to vacuum electromagnetic field.

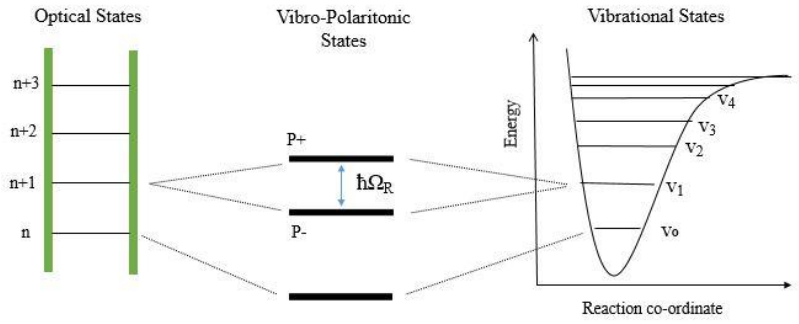

Figure 1.5: Schematic diagram of the strong coupling of the vibrational states of the molecule leads to the formation of "Vibro-Polaritonic" states.

Under VSC, the vibrational excited state (V_1) is coupled to one of the optical mode leads to the formation of vibro-polaritonic states. The formation of vibro-polaritonic states can be characterized from the vibrational spectra of molecule inside the cavity (figure 1.6). The Cyanide (-CN) stretch of bare "Benzonitrile" positioned at 2230 cm^{-1}, when molecule is placed inside cavity, in infrared spectrum the –CN stretch of the "Benzonitrile" splits in two peaks (lower energy peak is designated as P- while the higher wavenumber peak P+), as the V_1 state splits into two states now the transition can take place to both the states which results in two peaks. At ON-resonance condition the energy spacing P+ and P- from the original absorption peaks is same and they are equal in intensity (this changes with spectral shape). Here, Rabi splitting of 48 cm^{-1} is observed.

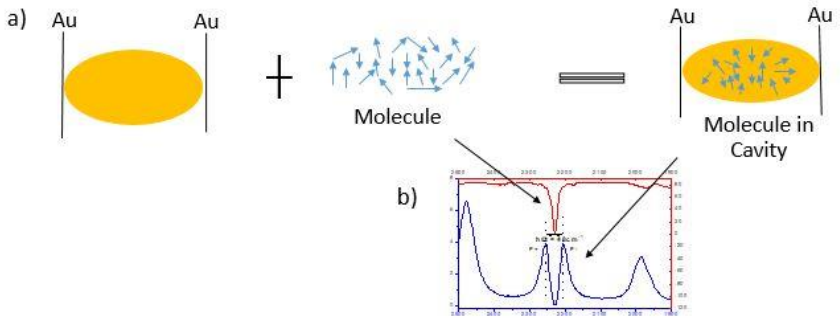

Figure 1.6: a) Schematic diagram of a cavity formed by two gold mirrors, transition dipoles of molecules shown by arrows and the molecules inside the cavity (also known as dressed molecules). b) IR spectra of bare benzonitrile (red trace), IR spectra of ON-resonance VSC of benzonitrile (blue trace).

As discussed above not only the energy of the excited state changes but also the energy of ground state. This change occurs even in the dark (absence of light) because of the vacuum field, so the chemical properties can be expected to modify by simply placing molecule inside an F–P cavity (i.e. no electromagnetic field is applied). The shift of the ground level of coupled system was first predicted (planar micro cavity-intersubband transition of semiconductor)[37] and later observed (LC resonator magnetically coupled to super-conducting qubit)[38] for systems under ultrastrong coupling. For organic molecules, the first experimental observation of the modification of ground state thermodynamics happened in 2013[39]. The thermodynamics of a planner cavity-molecules coupled system was studied by considering the equilibrium state between coupled (C) and uncoupled (U) molecules. The equilibrium constant ($K = [C]/[U]$) which can be calculated from the fluorescence and absorption spectra. The standard Gibbs free energy difference (ΔG_C) between the ground states of coupled and uncoupled molecules can be further obtained using

$$\Delta G^{\circ}_{C} = -k_B T ln K \tag{1.9}$$

where k_B and T are Boltzmann's constant and temperature respectively.

As discussed above, VSC can modify the vibrational landscape which in turn leads to modification of chemical properties. The main concept of the current project is to look in the effect of VSC on controlling the electronic structure as well as the influence of solvent systems that can control the photophysical properties of a solvent sensitive probe.

Chapter 2: Experimental results

2.1 Experimental methods to achieve vibrational strong coupling (VSC) regime:

As discussed previously, an essential condition for a system to undergo (VSC) is that, the reversible exchange of energy, between the bond dipole (molecule) and an electromagnetic mode of a cavity. This exchange process must be faster than any other energy dissipation process in the system. The very important condition for reversible exchange of energy is the energy of the electromagnetic mode has to be ON-resonance with that of the molecular transition (electronic or vibrational) energy. F-P cavities with two parallel mirrors placed roughly 6 to 12 μm form an IR cavity (fig 2.1), which can be used for the proposed studies.

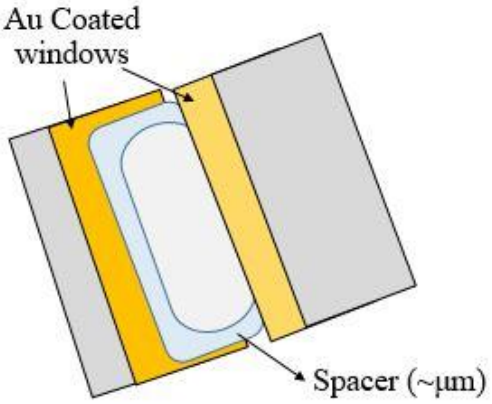

Figure 2.1: Schematic diagram of an F–P cavity, barium fluoride (BaF_2) substrates are coated with gold (Au) mirror separated by a Mylar spacer of 2 to 12 μm length.

The F-P cavity consist of the two barium fluoride (BaF_2) windows coated with gold (Au) mirrors place parallel to each other so that light can bounce back and forth between the mirrors forming a standing wave pattern. At resonance condition the cavity length, L_{cav} is equal to the integral multiple of intra-cavity wavelengths.

$$L_{Cav} = m(\frac{\lambda}{2n}) \tag{2.1}$$

where m, λ and n are integer number, wavelength of light and the refractive index of the medium inside the cavity. The energy dissipation from the cavity (from absorption, scattering or leakage through the imperfect mirrors) is characterized by the quality factor (Q-factor)[7]:

$$Q = \frac{\omega_r}{\Delta\omega_c} \tag{2.2}$$

where ω_r and $\Delta\omega_c$ are the resonant frequency and the linewidth (FWHM) of the cavity mode respectively. To achieve strong coupling the Q factor of the cavity must be high.

For studying the strong coupling as discussed earlier, mirrors are usually made on IR transparent substrate, (transparency varies for the transition to be coupled like glass, quartz, CaF_2, ZnSe etc. in the infrared). Then the active layer is dispersed on the mirror by various process either by sputtering or spin-coating. Organic molecules (chromophore) are commonly dispersed into an inert matrix (e.g. polymer) and then spin coated to form a film[7]. Then this layer is sputtered with a top Au mirror to achieve an F–P cavity configuration. Thus the thickness of the active layer determines the length of the F – P cavity.

All the experiment performed in the current thesis, the active medium is a molecular liquid. For VSC the cavity length are in the order of μm and the other advantage of having liquid is that the effective cavity length can adjust preciously by moving the top mirror in a "micro-fluidic cell" configuration (figure 2.2). Solution can be injected into the microfluidic cavity and further spectroscopy can done either in static or in flow conditions.

Figure 2.2: Picture of a microfluidic cavity used for VSC. The length of the cavity formed is in the range of 6 – 12 μm.

Transmission IR spectrum of an F-P cavity is shown in figure 2.3. The cavity mode formed are well separated and uniformly placed. As the cavity act as a harmonic oscillator, the optical modes are separated equally, as evident in the IR spectrum. The energy difference between the optical modes is known as "Free spectral range (FSR)" and it's calculated from equation (12)

$$FSR = \frac{10{,}000}{2nl} \tag{2.3}$$

where n is the refractive index of the medium and L is the length of the cavity. The FSR is not only the energy difference in the optical modes but also it is the energy of the first optical mode. Once the active layer is injected into the cavity the n changes as that of medium, but with the microfluidic cell there is a liberty of varying the length of cavity so as to couple a band of interest. One can pre-set and ON-Resonance condition by knowing the FSR, an integral multiple of FSR will have exactly matching energy to the molecular transition energy.

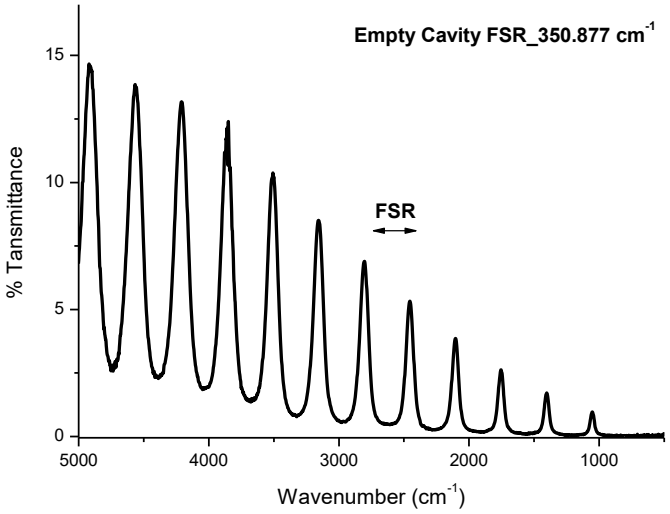

Figure 2.3: IR spectra of empty cavity with FSR = 350.877 cm^{-1}.

Thus by vibrational strong coupling it's possible to modify the chemical reactivity of molecule by strongly coupling the band responsible for the reaction to proceed. In order to explore more aspects of the VSC some experiments have been carried out to understand and modulate system accordingly.

2.2 Solvent sensitive Probes

Several studies on various chromophoric systems has revealed that the chemical equilibria, rates-kinetics of chemical reactions, position of spectral band are observed to be dependent on solvent medium[41]. The very first report on solvent dependence was reported by Berthelot and Pean de Saint-Gilles in 1862 where they have discussed their studies on esterification of acetic acid with ethanol, it was observed that the esterification is disturbed and decelerated on addition of neutral solvents not belonging to the reaction[42].

These difference in intermolecular interactions are broadly classified in two categories:

(i) Specific interactions = These include electron donor-acceptor activity (between electron-pair donor (EPD) and electron-pair acceptor (EPA)), solvophobic, H-bonding interactions (between H-bond donor (HBD) and H-bond acceptor (HBA))

(ii) Non-Specific interactions = These includes purely electrostatic interaction arising from Columbic interactions between charged ions and dipolar molecules (ion-ion,

ion-dipole, dipole-dipole) and polarisation interactions which depends on the solvent and solute intrinsic parameters such as dipole moment (μ), dielectric constant (ε) and refractive index of the medium[51-53].

To take all these terms into consideration "Reichardt" proposed term "*polarity*" for "*Overall solvent capability"*, this doesn't include the solvent-solute interactions which leads to permanent change in chemical structure of the molecules. Many compounds shows significant shift in the UV-Vis band on changing solvent, this phenomenon is known as *"Solvatochromism"*. Solvatochromism can be of two types.

a) Positive Solvatochromism: This is shown by the molecules those have less polar ground state compared to more polar excited state. On increasing solvent polarity, excited state stabilizes more as compared to ground state because of the more polar excited state. This leads to decrease in the transition energy, increase in absorption maxima (λ_{max}) on increasing solvent polarity (fig 2.4).

b) Negative Solvatochromism: This is observed among the molecules having more polar ground state compared to that of the less polar excited state. On increasing solvent polarity, the ground state stabilizes more compared to excited state which leads to increase in transition energy and decrease in absorption maxima (λ_{max}) on increasing solvent polarity.

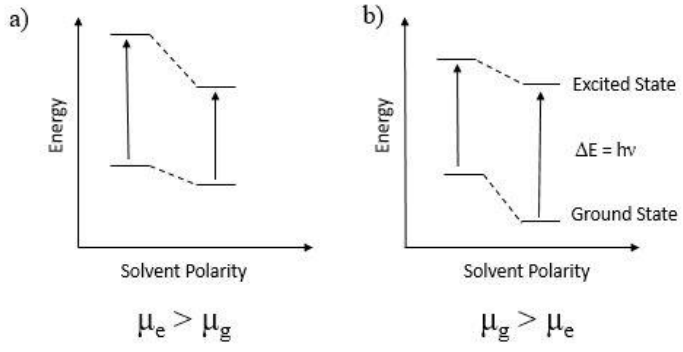

Figure 2.4: Schematic diagram of a) Positive solvatochromism and b) Negative Solvatochromism.

2.3 Fluorescence of 1,8-ANS

Anilinonapthalenesulphonates (ANS) molecules are of great interest particularly for their biological applications. The very first report of the ANS was in 1954 by Weber and Laurence[57], in which they have discovered the fluorescent behaviour of 1,8-ANS and its derivative 2,6-ANS (fig 2.5), depending on the solvent composition, in particular solvent polarity. They have observed the fluorescence of these two probes decreases drastically in water while it is highly fluorescent when combined with albumin, dissolved in nonpolar organic solvents or isolated in solid form[58]. This environment-sensitive fluorescence of 1,8-ANS attracted many who interested in biological problems, the ANS derivatives were used to measure the binding capacity of serum albumin[59], to evaluate "polarity" of protein and enzyme binding sites[60-62].

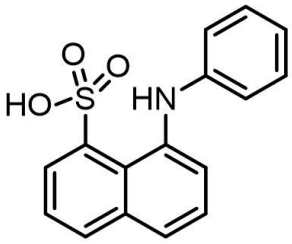

Figure 2.5: Structure of 1,8-ANS

There had been extensive photophysical studies on various ANS derivatives, but these does not explain the solvent sensitive behaviour[63]. In 1982 Edward. M. Kosower have projected a "two fluorescent state" theory for this solvent sensitive behaviour[58], in which they have studied the fluorescent behaviour of 2,6-ANS (derivative of 1,8-ANS) Two correlation lines are observed when fluorescence energies of different substituents of 2,6-ANS are plotted versus the E_T30 (corresponding to polarity) energies as shown in figure 2.6 (a). Two correlation lines can't be formed from one excited state, it was concluded that there are two fluorescence state (excited) of ANS which giving rise to different correlation. This was further confirmed by plotting fluorescence quantum yield (φ_F) versus the solvent polarity energies ($E_T(30)$) (fig 2.6 (b)) .

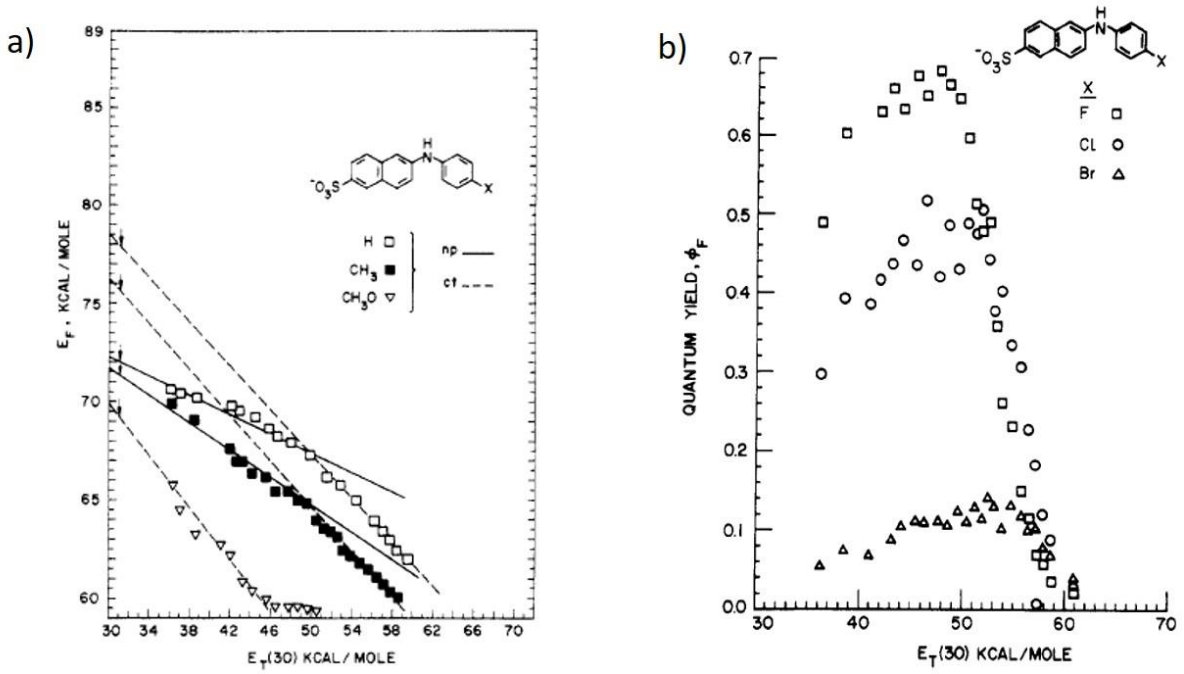

Figure 2.6: a) Plot of E_F (fluorescence energy) V/S the solvent polarity (E_T (30)) for 2,6-ANS. b) Plot of φ_F (fluorescence quantum yield) V/S the solvent polarity (E_T(30)) for 2,6-ANS. Figures are taken from ref. 64

It was observed that the E_F varies modestly with the non-polar solvent, this happen through a locally excited state (labelled as $S_{1,np}$). For high polarity E_F varies drastically (having slope of 0.65) due the decay rates are happening through a charge transfer (Fig 2.7 (labelled as $S_{1,ct}$)). Second evidence for the for the two decay channels of 1,8-ANS in glycerol correspond to $S_{1,np}$ emission in spite of high polarity of solvent[68]. The high viscosity of glycerol inhibits the formation of charge-transfer state. Other viscous and rigid media permits emission only from $S_{1,np}$ state.

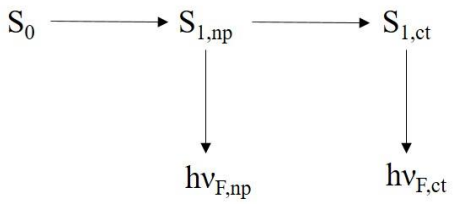

Figure 2.7: Schematic diagram of the fluorescence channels of ANS from two excited state.

From pure ethanol to pure water the k_R (radiative rate constant) decreases (by a factor of 3) while k_{NR} (non-radiative decay) increases by a factor of 75[65]. The fluorescence quantum yield of 1,8-ANS decreases by a factor of 100 on going from ethanol to water when $E_T(30)$ changes only from 52 to 63[66], the same result is obtained on going from pure dioxane to pure water as $E_T(30)$ changes from 36 to 63[67].

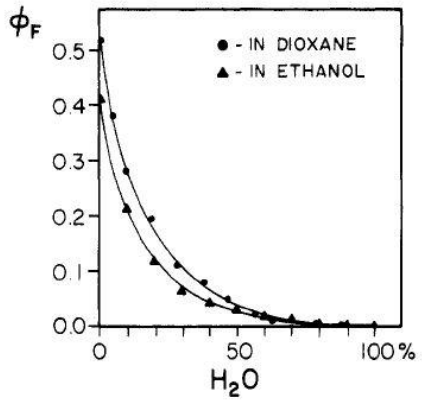

Figure 2.8: Fluorescence quantum yield of 1,8-ANS in various composition of Dioxane-Water mixture and Ethanol-Water. Taken from ref. 66 & 67.

2.4 VSC of 1,8-ANS in water-dioxane mixture:

In the previous section, we discussed that 1,8-ANS has different radiative and non-radiative decay rates from the two excited states. Our main goal in the current project is to understand the effect of VSC on modifying the decay processes.. Here, we have tried VSC of the O-H stretch of water (~3500 cm^{-1}) that could in principle modulate the radiative and non-radiative decay rates of 1,8-ANS as water is playing an important role in controlling the non-radiative decay rates of ANS in Dioxane-water mixture. Another interesting feature of 1,8-ANS is that the availability of an O-H stretch mode (~3200 cm^{-1}) (fig 2.9) near to water O-H stretch, this gives a chance of other secondary effect to control the decay kinetics due to external vibrational relaxation (EVR) through these vibrational modes (fig 2.10). Dioxane and water has same boiling point, whereas the solvation energies are completely different. The concentration of 1,8-ANS was maintained ~ 7.16 mM in all the further measurements.

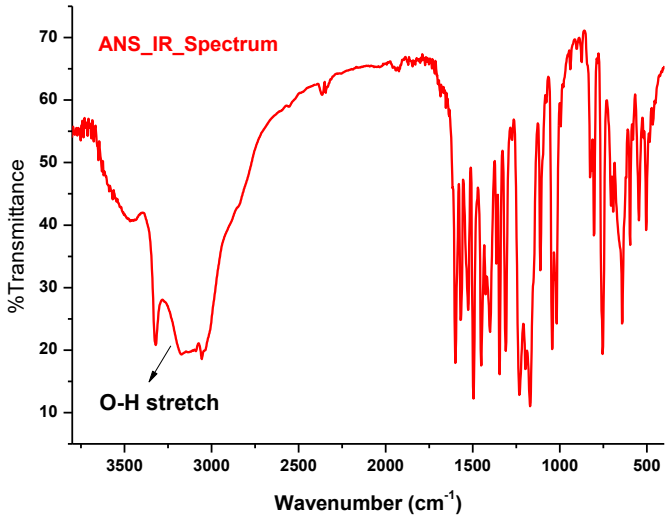

Figure 2.9: FTIR spectrum of 1,8-ANS (recorded in KBr pellet).

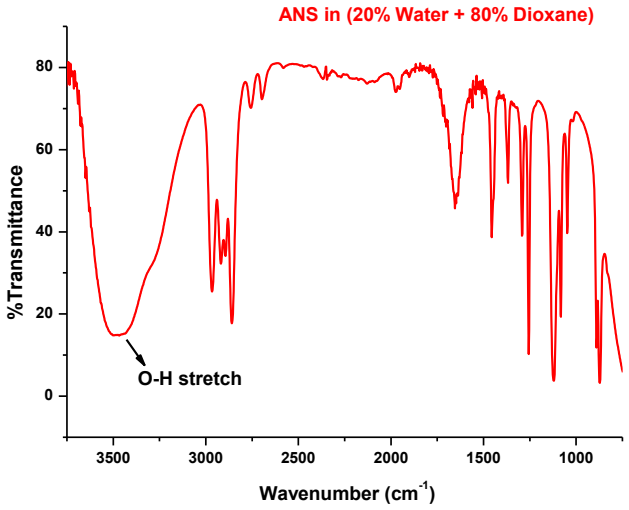

Figure 2.10: FTIR spectrum of 1,8-ANS in 20%Water + 80%Dioxane.

For VSC, the O-H stretching mode of the water was strongly coupled to the 7th mode of an F–P cavity. Here, F–P cavity was formed by sputtering ~10 nm gold layer on barium fluoride (BaF_2) substrates, and cavity length was maintained by using a Mylar spacer of ~ 7 μm. In order to examine the fluorescence behaviour of 1,8-ANS in dioxane-water mixtures under vibrational strong coupling, various dioxane-water composition was taken and fluorescence data were recorded (table 2.1). The alterations in the fluorescence behaviour of 1,8-ANS observed in each case is discussed below which are further analysed in section 2.5.

Concentration Of 1,8-ANS (µM)	Concentration Of 1,4-Dioxane (%)	Concentration Of Water (%)
7.16	100	0
7.16	95	5
7.16	90	10
7.16	75	15
7.16	80	20

Table 2.1: Concentration of 1,8-ANS, 1,4-Dioxane and Water used for study of fluorescence behaviour of 1,8-ANS under VSC of O-H stretch of water.

A) 1,8-ANS in (0%Water + 100%Dioxane):

We have started the experiment with pure dioxane containing 1,8-ANS in the F-P cavity. At first, solution of 1,8-ANS was prepared in 1,4-Dioxane (spectroscopic grade), then the solution was injected into microfluidic cell or cavity. Cavity mode was tuned to 3500 cm-1 and fluorescence data was recorded (fig 2.11). Empty cavity was tuned to FSR = 705 cm^{-1} and after injecting solution into cavity FSR changes to 500 cm^{-1}, such that the 7^{th} mode of cavity (500 x 7 = 3500) will reach the region of interest for the current studies.

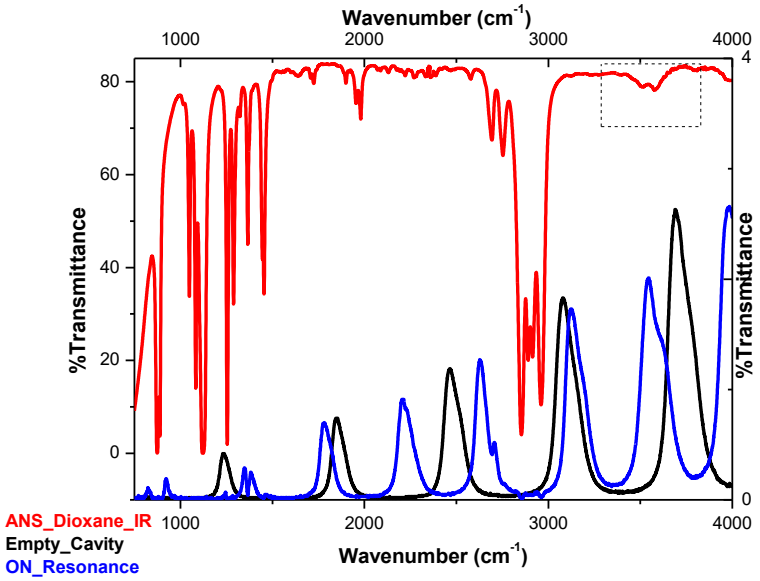

Figure 2.11: FTIR spectrum of 1,8-ANS in (0%Water + 100% Dioxane). The dash boxed region shows the expected position of O-H stretch of the water molecule (but here there is no water), small absorption in the dashed region corresponds to the O-H stretch of 1,8-ANS.

Under the above conditions, fluorescence spectra were recorded in the Cell and tuning to 3500 cm-1 (ON resonance with respect to O-H stretching of water)in an F-P cavity (fig 2.12). Here, cell or the non-cavity is the same microfluidic cell without any mirrors in it. Fluorescence spectral measurements were acquired at 23 degree incident angle (front face measurement mode) in a Shimadzu fluorimeter (model No. RF 500). The emission spectra for both the cases (cell and ON-resonance) recorded at λ_{exc} = 370 nm with excitation slit = 5 nm and emission slit width = 3 nm. Emission maxima for the cell was observed at 476 nm (black trace) while for ON resonance cavity condition was observed at 480 nm (red trace). While the excitation spectra in cell was recorded with excitation slit and emission slit width at 5 nm, λ_{ems} = 476 nm and excitation maxima was observed at 370 nm.

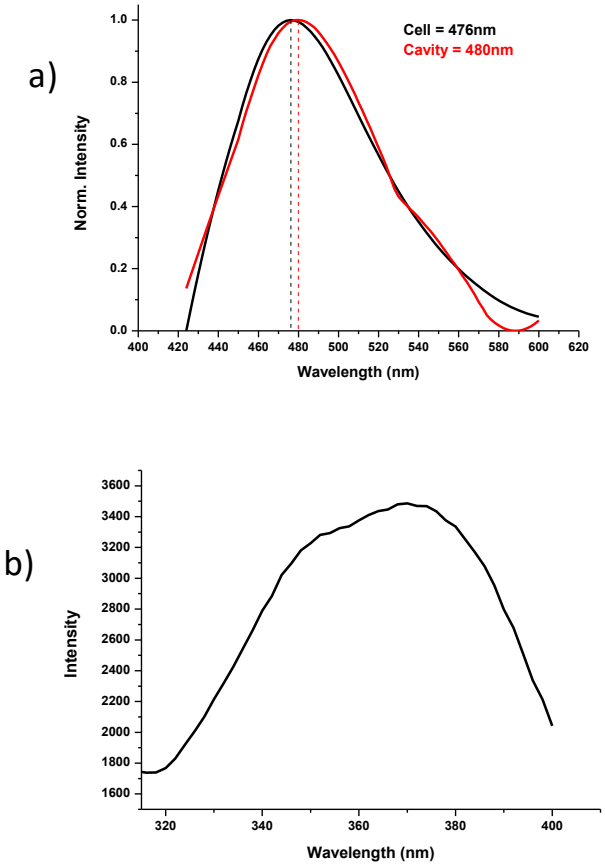

Figure 2.12: a) Normalized fluorescence (emission) spectra of 1,8-ANS in pure dioxane (or 0%Water +100%Dioxane mixture). The emission maxima for the ON resonance condition shows a red shift of 4nm compared to that of non-cavity (cell) condition. b) Excitation spectra of 1,8-ANS in pure dioxane (recorded in cell).

B) 1,8-ANS in (10% Water + 90% Dioxane):

The O-H stretch (of water) band in this solution mixture positioned at 3510 cm^{-1}. Refractive index of medium (10% Water + 90% Dioxane) is 1.411, so empty Cavity was tuned to FSR = 706 cm^{-1} such that after injection of solution the FSR of the cavity shifted to 501.35 cm^{1} (because as the refractive index of medium changes from 1 to 1.411 (as discussed in equation 2.3), Now the 7^{th} mode of cavity will have energy equivalent to energy of O-H bond (as 501.35 x 7 = 3509.45). VSC of O-H stretch of water (10%) gives vibro-polaritonic states P+ = 3625 cm^{-1} and P- = 3415 cm^{-1} and the observed Rabi splitting = $\hbar\Omega_R$ = 210 cm^{-1} and the %splitting energy = 5.98% (as shown in figure 2.13).

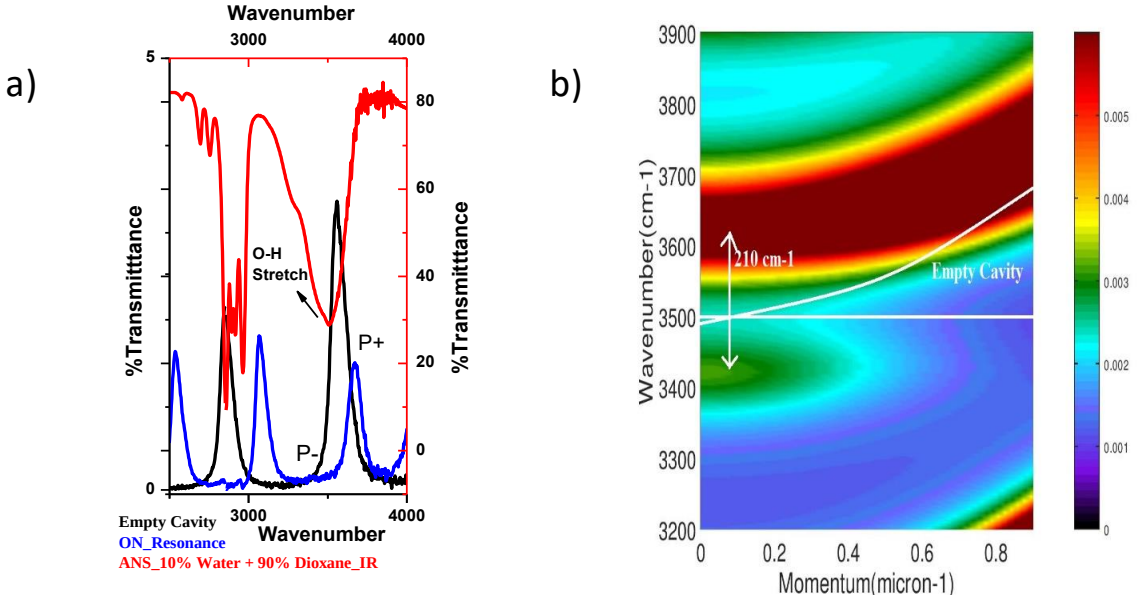

Figure 2.13: a) FTIR spectrum of ANS in (10% Water + 90% Dioxane) (red trace), IR spectra of empty cavity (black trace) and ON resonance (blue trace), P- is low intensity. b) In order to confirm the VSC dispersion curve of vibro-polaritonic states P+ and P- is obtained. Rabi splitting is calculated from the difference in energies of middle of P+ and P-.

After the system is under VSC condition fluorescence studies were done and compared to that of the non-cavity condition. First, excitation spectra for both the cases (cell and ON-resonance) were recorded with λ_{ems} = 475 nm with excitation slit and emission slit width at 5 nm. The excitation maxima for cell was observed at 358 nm (black trace) while for ON resonance cavity

condition was observed at 352 nm (red trace). Fluorescence spectral shift is observed in cavity (ON-resonance) compared to that of non-cavity condition, the nature of shift in both cases are different (fig 2.14 (a)).

A clear blue shift is observed in the excitation spectra of approx. 6 nm (~ 476.13 cm^{-1}) while in emission spectra a red shift of approx. 6 nm (~ 253 cm^{-1}) was observed. The emission maxima for cell was at 484 nm (black trace) while for ON resonance cavity condition was at 490 nm (red trace). The emission spectra for both the cases recorded at λ_{ems} = 375 nm with excitation slit and emission slit width at 5 nm (fig 2.14 (b)).

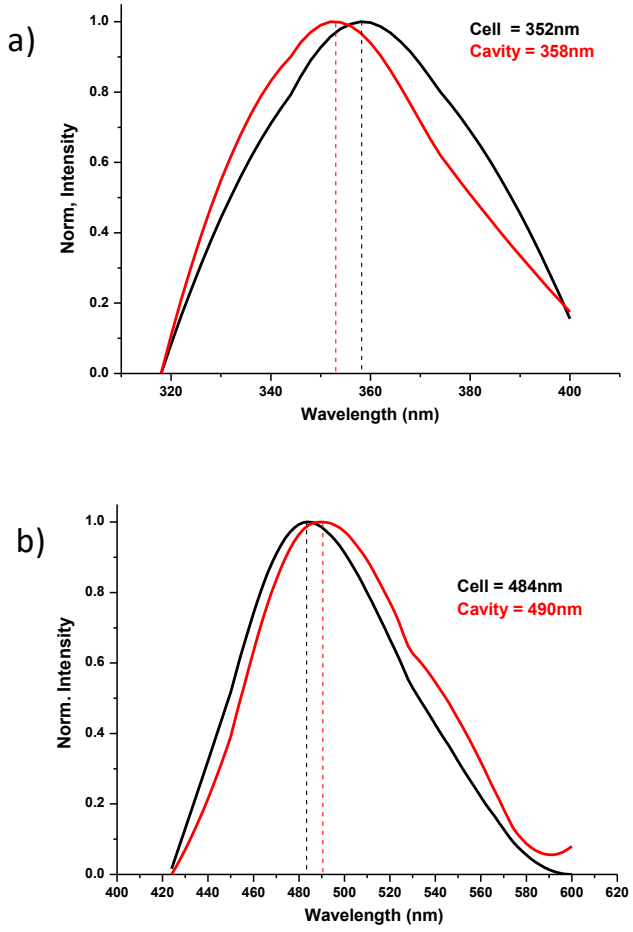

Figure 2.14: a) Normalized fluorescence (excitation) spectra of 1,8-ANS in 10%Water + 90%Dioxane mixture. b) Normalized fluorescence (emission) spectra of 1,8-ANS in 10%Water + 90%Dioxane mixture).

2.5 Data Analysis:

The above studies were performed for the five different sets of concentration (table 2.1). As discussed in the 1st chapter one predominant feature of strong coupling is that Rabi splitting is directly proportional to the square root of concentration. A similar correlation was observed in the current studies as well. (Fig 2.15).

Conc" of Water (%)	Conc" of Water (M)	$\sqrt{C}$ ($M^{1/2}$)	P+ (cm^{-1})	P- (cm^{-1})	hΩ (cm^{-1})
5	2.775	1.666	3471	3606	135
10	5.55	2.35	3625	3415	210
15	8.325	2.885	3659	3380	279
20	11.1	3.33	3709	3354	355

Table 2.2: Values of energies of polaritonic states, concentration of water in different mixtures of dioxane-water and Rabi splitting energy.

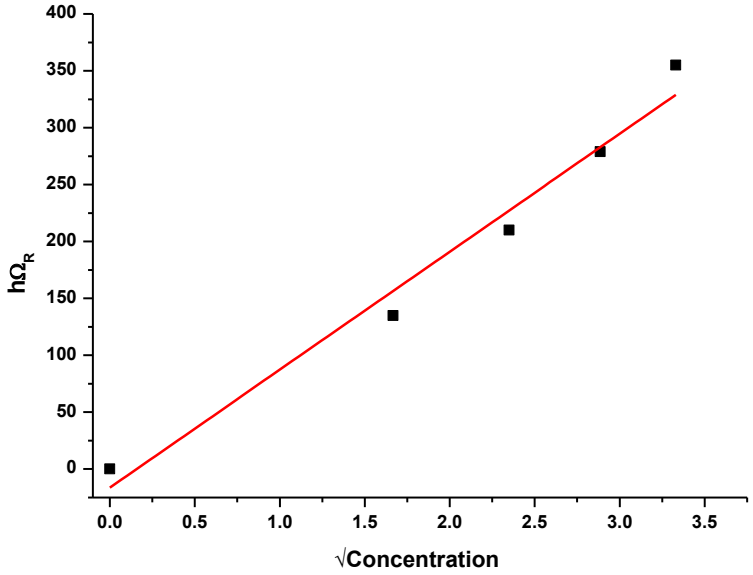

Figure 2.15: Linearly fitted graph of Rabi splitting versus √Concentration. Directly proportionality relation is followed.

As discussed in section 2.4.2, a red shift (in the ON-resonance compared to cell condition) in the fluorescence (emission) spectra of 1,8_ANS in the various set of the ON-resonance condition measurements compared to that of emission maxima of cell condition was observed (Table-2.3). The E_F (fluorescence energy) of 1,8-ANS was plotted with the E_T30 (solvent polarity parameter) as on changing water concentration the polarity of solvent changes(fig-2.16) and this was plotted with respect to the Rabi splitting energy (fig 2.17).

Conc. of Water (M)	E_T 30 Values (kcal mol^{-1})	Δλ (nm)	Δλ (cm^{-1})	ΔE (kcal mol^{-1})
0	36	4	175.08	0.501
2.775	37.355	6	255.71	0.729
5.5	38.71	8	335.93	0.96
8.3	40.065	11	455.41	1.302
11.1	41.42	14	576.13	1.647

Table 2.3: Values of E_T30 of different concentration of water in different sets with the energies of red shift observed in the emission spectra of 1,8-ANS.

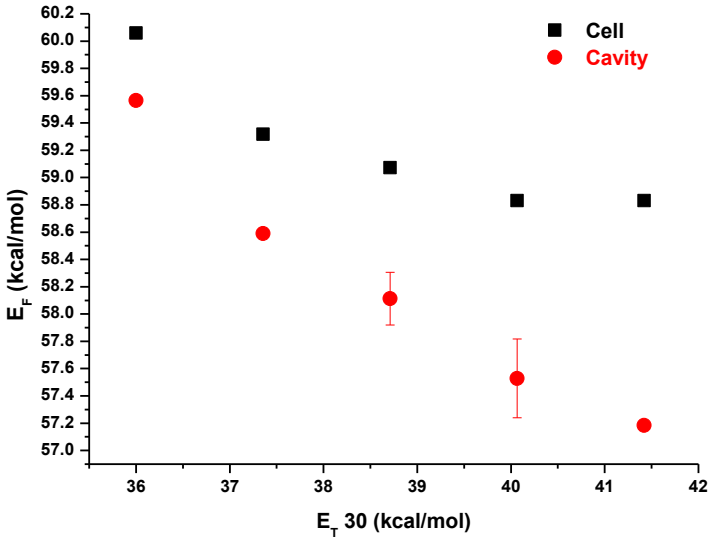

Fig 2.16: Plot of Fluorescence energy (E_F) of 1,8-ANS with respect to solvent polarity parameter (E_T30). Black squares corresponds to the fluorescence energies recorded in cell while the red circles correspond to energies recorded in ON resonance cavity condition.

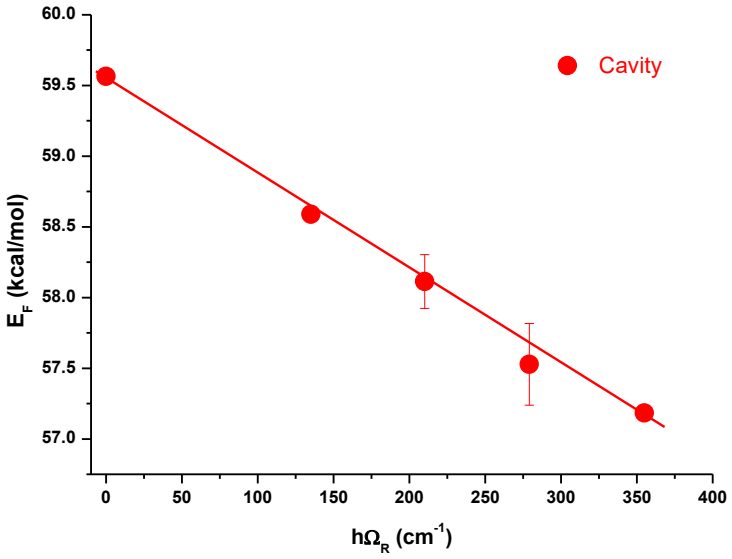

Fig 2.17: Plot fluorescence energy (E_F) of 1,8_ANS with respect to the Rabi splitting.

A clear change in the fluorescence energy (E_F) energy of 1,8-ANS is observed as shown in figure 2.17 and it decrease linearly with increasing Rabi splitting of water vibro-polaritonic states. The energy modification (ΔE_F) is also observed to be linearly dependent on E_T30 values of the various solvent mixtures, while in the non-coupled situation (when $\hbar\Omega_R$ is zero for pure dioxane) shows a deviation from the linear fitting (fig 2.18 and 2.19).

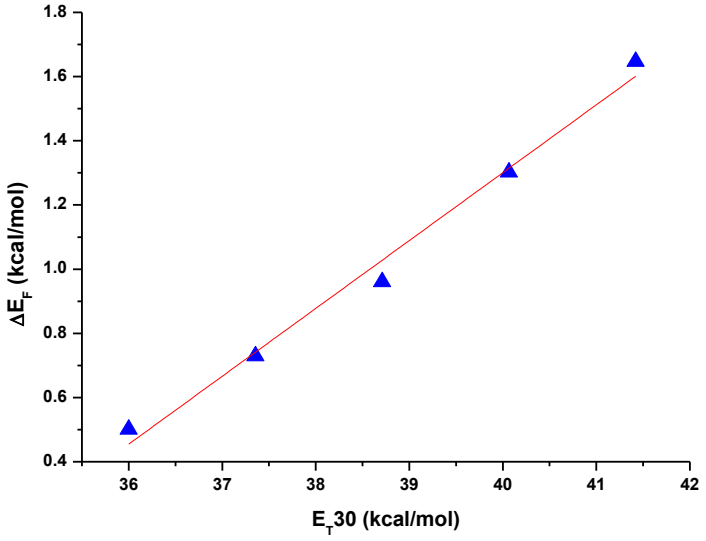

Fig 2.18: Linearly fitted plot of fluorescence energy (of 1,8-ANS) shift with respect to solvent polarity (E_T30).

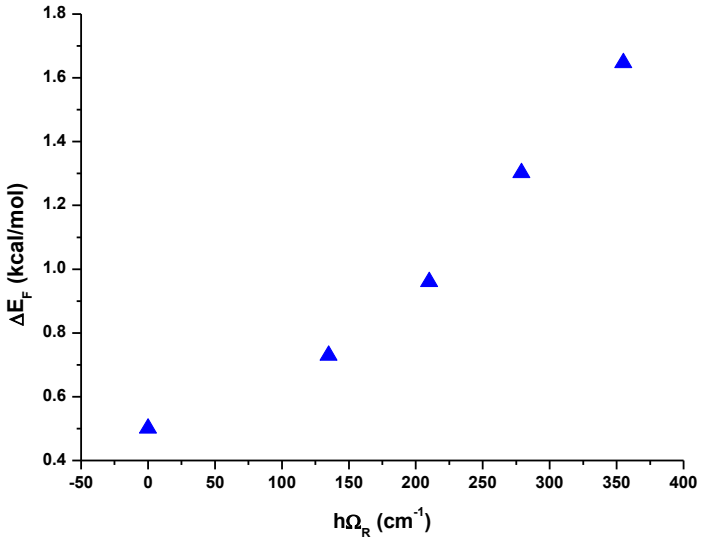

Fig 2.19: Plot of ΔE_F for 1,8-ANS with respect to observed Rabi splitting.

2.6 Conclusion:

In conclusion, the electronic transition energy of a solvent sensitive probe is modified by VSC of solvent molecules. Here, we have strongly coupled O-H stretching band of water molecule which in turn shows the modification in the fluorescence spectra of 1,8-ANS molecules. Concentration dependant studies show that a bathochromic shift in the emission is linear with respect to VSC strength. Similarly, a hypsochromic shift in the action spectra is observed in the strongly coupled system. The above observations show that the bulk polarity of solvent system is affected under VSC. It can also be due to modification of intermolecular interaction between solvent and probe under strong coupling conditions. Further studies such as fluorescence polarization anisotropy and lifetime measurements are required to fully understand this fundamental behaviour of electronic structure modification. These experiments open up a new platform to study the effect of modification of intrinsic behaviour of chromophoric systems under light-matter strong coupling.

References

1. Forster, S.T, *Ann. Physik*., 2, 55 **(1948)**.
2. T. Kobayashi, J-aggregates, *World Scientific*, **2012**.
3. K. H. Drexhage, in Progress in Optics, ed. E. Wolf**,** *Elsevier,**1974***, vol. 12, pp. 163–232.
4. E. M. Purcell, H. C. Torrey and R. V. Pound, *Phys. Rev.*,**1946**, 69, 37–38.
5. V. A. Yakovlev, V. G. Nazin and G. N. Zhizhin, *Opt. Commun.*,**1975**, 15, 293–295.
6. W. T. Simpson and D. L. Peterson, *J. Chem. Phys.*, **1957**, 26,588–593.
7. M. Hertzog, M. Wang, J. Mony. K. Borjesson, **2018**, *Chem. Sco. Rev*.
8. M. Planck, Verh. Dtsch. *Phys. Ges.*, **1911**, 13, 138–148.
9. A. Einstein and O. Stern, *Ann. Phys.*, **1913**, 345, 551–560.
10. E. T. Jaynes and F. W. Cummings, Proc. *IEEE*, **1963**, 51, 89–109.
11. J. J. Hopfield, *Phys. Rev*., **1958**, 112, 1555–1567.
12. T. W. Ebbeson, *Acc. Chem. Res.* **2016**, 49, 2403−2412.
13. R. Houdre, R.P. Stanley, M. Ilegems, Phys. Rev. A: Mol, *Opt. Phys*. **1996**, 53, 2711-2715.
14. S. Aberra Guebrou, C. Symonds, E. Homeyer, J. C. Plenet, Y. N. Gartstein, V. M.Agranovich, and J. Bellessa, *Phys. Rev. Lett*. **2012**, 108, 066401.
15. L. Shi, T. K. Hakala, H. T. Rekola, J. P. Martikainen, R. J. Moreland and P. Torma, *Phys. Rev. Lett.* **2014**, 112, 153002.
16. S. Wang, T. Chervy, J. George, J. A. Hutchison, C. Genet and T. W. Ebbesen, J. *Phys. Chem. Lett*. **2014**, 5, 1433−1439.
17. R. Houdre´, R. P. Stanley and M. Ilegems, Phys. Rev. A: At., Mol., *Opt. Phys*., **1996**, 53, 2711–2715.
18. P. R. Rice and R. J. Brecha, *Opt. Commun.*, **1996**, 126, 230–235.
19. H. Tanji-Suzuki, W. Chen, R. Landig, J. Simon and V. Vuletic´, *Science*, **2011**, 333, 1266–1269.
20. W. Zhao, S. Wang, B. Liu, I. Verzhbitskiy, S. Li, F. Giustiniano, D. Kozawa, K. P. Loh, K. Matsuda, K. Okamoto, R. F. Oulton and G. Eda, *Adv. Mater.*, **2016**, 28, 2709–2715.

21. C. Ciuti, G. Bastard and I. Carusotto, Phys. Rev. B: *Condens. Matter Mater. Phys.*, **2005**, 72, 115303.
22. M. A. Bastarrachea-Magnani, S. Lerma-Herna´ndez and J. G. Hirsch, *Phys. Rev. A*: *At., Mol., Opt. Phys*., **2014**, 89, 032101.
23. A. Ridolfo, M. Leib, S. Savasta and M. J. Hartmann, *Phys. Rev. Lett*., **2012**, 109, 193602.
24. C. Hamsen, K. N. Tolazzi, T. Wilk and G. Rempe, *Phys. Rev. Lett.*, **2017**, 118, 133604.
25. A. Vasanelli, Y. Todorov and C. Sirtori, *C. R. Phys.*, **2016**, 17, 861–873.
26. T. Jaako, Z.-L. Xiang, J. J. Garcia-Ripoll and P. Rabl, *Phys. Rev. A*: *At., Mol., Opt. Phys.*, **2016**, 94, 033850.
27. L. A. Martı´nez-Martı´nez, R. F. Ribeiro, J. Campos-Gonza´lez-Angulo and J. Yuen-Zhou, *ACS Photonics***, 2018**, 5, 167–176.
28. D. Ballarini, M. De Giorgi, S. Gambino, G. Lerario, M. Mazzeo, A. Genco, G. Accorsi, C. Giansante, S. Colella, S. D'Agostino, P. Cazzato, D. Sanvitto and G. Gigli, *Adv. Opt. Mater*., **2014**, 2, 1076–1081.
29. T. Grant Richard, P. Michetti, J. Musser Andrew, P. Gregoire, T. Virgili, E. Vella, M. Cavazzini, K. Georgiou, F. Galeotti, C. Clark, J. Clark, C. Silva and G. Lidzey David, *Adv. Opt. Mater*, **2016**, 4, 1615–1623.
30. H. Bahsoun, T. Chervy, A. Thomas, K. Bo¨rjesson, M. Hertzog, J. George, E. Devaux, C. Genet, J. A. Hutchison and T. W. Ebbesen, *ACS Photonics*, **2018**, 5, 225–232.
31. T. Schwartz, J. A. Hutchison, C. Genet and T. W. Ebbesen, *Phys. Rev. Lett***., 2011**, 106, 196405.
32. J. A. Hutchison, T. Schwartz, C. Genet, E. Devaux and T. W. Ebbesen, *Angew. Chem., Int. Ed***., 2012**, 51, 1592–1596.
33. A. Shalabney, J. George, J. Hutchison, G. Pupillo, C. Genet and T. W. Ebbesen, *Nat. Commun.*, **2015**, 6, 5981.
34. J. P. Long and B. S. Simpkins, *ACS Photonics*, **2015**, 2,130–136.

35. T. Chervy, A. Thomas, E. Akiki, R. M. A. Vergauwe, A. Shalabney, J. George, E. Devaux, J. A. Hutchison, C. Genet and T. W. Ebbesen, *ACS Photonics*, **2018**, 5, 217–224.
36. R. M. A. Vergauwe, J. George, T. Chervy, J. A. Hutchison, A. Shalabney, V. Y. Torbeev and T. W. Ebbesen, *J. Phys. Chem. Lett*., **2016**, 7, 4159–4164.
37. C. Ciuti, G. Bastard and I. Carusotto, Phys. Rev. B: *Condens. Matter Mater. Phys.*, **2005**, 72, 115303.
38. P. Forn-Dı´az, J. Lisenfeld, D. Marcos, J. J. Garcı´a-Ripoll, E. Solano, C. J. P. M. Harmans and J. E. Mooij, *Phys. Rev. Lett.*, **2010**, 105, 237001.
39. A. Canaguier-Durand, E. Devaux, J. George, Y. Pang, J. A. Hutchison, T. Schwartz, C. Genet, N. Wilhelms, J. M. Lehn and T. W. Ebbesen, *Angew. Chem*., **2013**, 125, 10727–10730.
40. K. J. Vahala, *Nature*, **2003**, 424, 839–846.
41. C. Reichardt, *Chem. Soc. Rev.*, **1992,** 147–153.
42. M. Berthelot, Pean de Saint-Gilles, *L. Ann. Chim. Phys.* **3.** Ser. **1862**, 65, 385-422; 1862, 66, 5-110; 1863, 68, 255-359.
43. C. Machado, V. G. Machado, *J. Chem. Edu.* **2001**, 78, 5.
44. D. B. Smithrud, F. Diederich, *J. Am. Chem. SOC.* **1990**, 112, 339-343.
45. D. B. Smithrud, T. B. Wyman, F. Diederich, *J. Am. Chem. SOC.* **1991**, 113, 5420-5426.
46. F. Diederich, Cyclophanes Monographs in Supramolecular Chemisty; J. F. Stoddart, Ed.; *Royal Society of Chemistry*: London, **1991**; Chapter 3**,** p 106 ff.
47. D. S. Kemp, K. G. Paul, *J. Am. Chem. SOC.***1975**, 97, 7305-7312.
48. D. S. Kemp, J. Reczek, F. Vellaccio, *Tetrahedron Lett.* **1978**, 741-742
49. J. W. Grate, R. A. McGill, D. Hilvert, *J. Am. Chem. SOC.* **1993**, 115, 8577-8584.
50. T. Scherer, W. Hielkema, B. Krijnen, R. M. Hermant, C. Eijckelhoff, F. Kerkhof, R. Verleg, A. M. Brouwer, J. W. Verhoeven, *Recl. Trav. Chim. Pays- Bas* **1993**, 112, 535-548.
51. A. D. Buckingham, P. W. Fowler, J. M. Hutson, *Chem. Rev.* **1988**, 88, 963-988.
52. P. L. Huyskens, W. A. P. Luck, T. Zeegers-Huyskens, *Eds. Intermolecular Forces; Springer: Berlin*, **1991.**

53. J. N. Israelachvili, Intermolecular and Surface Forces, *2nd ed.; Academic Press*: New York, **1992.**
54. a) C. Reichardt, Solvents and Solvent Effects in Organic Chemistry, *2nd ed; VCH: Weinheim*, **1988**; pp 285–405. (b) C. Reichardt, *Chem. Rev.* **1994**, 94, 2319–2358. (c) P. Suppan, N. Ghoneim, Solvatochromism; Royal Society of Chemistry: Cambridge, **1997**; Chapter 3.
55. K. Dimroth, C. Reichardt, T. Siepmann, F. Bohlmann, *J. Liebigs Ann. Chem.*, **1963**, 661, 1–37.
56. L. G. S. Brooker, G. H. Keyes, D. N. Heseltine, *J. Am. Chem. Soc.* **1951,** 73, 5350–5356.
57. G. Weber, D. J. Laurence, *J. R. Biochem.* **1954**, 56, 31P.
58. E. M. Kosower. *Acc. Chem. Res.* **1982**, 15, 259-266.
59. E. Danie, G. Weber, *Biochemistry***, 1966**, 5, 1893.
60. L. Stryer, *J. Mol. Biol*. **1965**, 13, 482-495.
61. D. C. Turner, L. Brand, *Biochemistry* **1968**, 7, 3381.
62. L. Stryer, Science (Washington, D.C.) **1968**, 162, 526-533.
63. C. Seliskar, L. Brand, *J. Am. Chem. Soc.* **1971**, 93, 5405-5414, 5414-5420.
64. E. M. Kosower, H. Dodiuk, K. Tanizawa, M. Ottolenghi, N. Orbach, *J. Am. Chem. SOC.* **1975**, 97, 2167-2178.
65. T. W. Ebbesen. C. A. Ghiron. *J. Phys. Chem.* **1989**, 93, 7139-7143.
66. G. W. Robinson, R. J. Robbins, G. R. Fleming, J. M. Morris, A. E. W. Knight, R. J. S. Morrison, *J. Am. Chem. SOC.* **1978**, 100, 7145.
67. E. M. Kosower, H. Kanety, *J. Am. Chem. SOC.* **1983,** 105, 6236.
68. E. M. Kosower, H. Dodiuk, *J. Am. Chem. SOC.* **1974**, 96, 6195-6196.
69. S. Kena-Cohen and S. R. Forrest, Phys. Rev. B: *Condens. Matter Mater. Phys*., **2007**, 76, 075202.
70. K. Stranius, M. Hertzog and K. Bo¨rjesson, *Nat. Commun.***2018**, 9, 2273.
71. L. H. Lin, M. S. Wang, X. L. Wei, X. L. Peng, C. Xie and Y. B. Zheng, *Nano Lett*., **2016**, 16, 7655–7663.
72. J. Feist, J. Galego and F. J. Garcia-Vidal, *ACS Photonics*, **2018**, 5, 205–216.
73. J. Galego, F. J. Garcia-Vidal and J. Feist, *Phys. Rev. X*, **2015**,5, 041022.

74. J. Galego, F. J. Garcia-Vidal and J. Feist, *Nat. Commun*. **2016**, 7, 13841.
75. J. Galego, F. J. Garcia-Vidal and J. Feist, *Phys. Rev. Lett*., **2017**, 119, 136001.
76. B. Munkhbat, M. Wersa¨ll, D. G. Baranov, T. J. Antosiewicz and T. Shegai, *Sci. Adv*., **2018**, 4, eaas9552.
77. J. George, A. Shalabney, J. A. Hutchison, C. Genet and T. W. Ebbesen, *J. Phys. Chem. Lett.* **2015**, 6, 6, 1027-1031.